Second-Kind Integral Formulations of the Capacitance Problem *

Johannes Tausch and Jacob White

September 22, 1997

Abstract

The standard approach to calculating electrostatic forces and capacitances involves solving a surface integral equation of the first kind. However, discretizations of this problem lead to ill-conditioned linear systems and second-kind integral equations usually solve for the dipole density, which can not be directly related to electrostatic forces. This paper describes a second-kind equation for the monopole or charge density and investigates different discretization schemes for this integral formulation. Numerical experiments, using multipole accelerated matrix-vector multiplications, demonstrate the efficiency and accuracy of the new approach.

1 Introduction

A classical problem in electrostatics is the determination of the charge density for a three-dimensional conductor system. For a given potential distribution f on the conductor surface(s) S this leads to the integral equation of the first kind

$$\int_S G(x,y)\sigma(y)\,dS_y = f(x)\,, \qquad x \in S \tag{1}$$

for the charge density σ. Here $G(x,y) = 1/4\pi|x-y|$ denotes the Green's function for the Laplacian in the three-space.

It is typical for applications in electrostatics that the surface is composed of several disconnected components $S = S_1 \cup \ldots \cup S_n$ (conductors or electrodes) and that the potential f is constant in each component, that is,

$$f(x) = \sum_{k=1}^{n} p_k \chi_k(x)\,, \qquad x \in S\,. \tag{2}$$

*This work is supported by the NSF under contract ECS-9301189

Here p_k is the potential on S_k and χ_k denotes the characteristic function of conductor surface S_k .

The capacitance matrix is an important parameter to determine the behavior of electric circuits. Its entry $C_{k,l}$ is defined to be the net-charge on S_k, if S_l is raised to one volt and all other conductors are grounded. Let $\sigma^{(l)}$ denote the solution of (1) with potentials $p_i = \delta_{l,i}$, then

$$C_{k,l} = \int_{S_k} \sigma^{(l)} \, dS \,, \quad 1 \leq k, l \leq n \,. \tag{3}$$

Sometimes the charge distribution σ as a function on the conductor is also of interest, because it is proportional to the electrostatic forces on the conductors.

For applications in complex geometries, integral equation (1) is usually discretized with a collocation scheme. The resulting matrices are dense and large. In the recent past, there has been an increased interest to sparsify this system, for instance with the fast multipole method. As a result, the matrix vector product can be carried out in $\mathcal{O}(N)$ operations and thus the solution of the linear system with an iterative scheme is feasible [6, 7, 8, 12].

The problem with the first-kind integral equation is that discretizations lead to matrices with increasing condition numbers as the mesh is refined. This behavior makes the solution of the linear system more expensive and more sensitive to errors due to multipole approximations. Furthermore, the numerical analysis of first-kind formulations is more difficult than for second-kind formulations. In particular, the theory of the collocation method is only well-understood for planar domains, but very little is known for three-dimensional problems (see, for example, Sloan [17]).

Many theoretical and practical difficulties associated with the first-kind formulation can be avoided by using a second-kind integral formulation for Laplace's equation. Typically, the arising integral operators are compact on smooth surfaces and thus the Riesz-Fredholm theory provides a framework for the analysis, see, e.g. [4]. Of particular importance are the asymptotic error estimates of discretizations which can be obtained this way. Also, the condition number of the discretized linear system can be bounded independently of the discretization mesh, and so require no preconditioning.

The capacitance problem is an exterior Dirichlet problem for the Laplace equation. Using double-layer potentials, this problem can be cast into a second-kind integral equation. The resulting operator has an n-dimensional nullspace which can be removed by augmenting the integral equation with n Lagrange multipliers, [1, 11]. The multipliers turn out to be the capacitances.

However, double-layer potentials do not yield the charge density as a function on the conductors. Since this is the quantity of main interest in many applications, we will derive a second-kind formulation which involves the adjoint of the double-layer operator and provides the charge density. For a similar approach along these lines see Atkinson [2].

The collocation method for the double-layer equation is well understood. Some of these results do not carry over to its adjoint and we will propose a modified collocation scheme to avoid these difficulties.

We will also demonstrate how the arising discretized linear systems can be sparsified with the fast multipole method and will conclude with several numerical examples comparing the different formulations.

2 Second-Kind Formulations

The idea behind the first-kind formulation is to set up the electrostatic potential as a single-layer potential of a surface charge

$$u(x) = \mathcal{V}\sigma(x) \equiv \int_S G(x,y)\,\sigma(y)\,dS_y\,, \quad x \in \mathbb{R}^3\,. \tag{4}$$

The single-layer potential satisfies Laplace's equation in every connected component of $\mathbb{R}^3 \setminus S$ and furthermore it is known that the single-layer potential is continuous in $\mathbb{R}^3$. Stipulating that u defined by (4) assumes the given values on the conductor surfaces, one obtains integral equation (1) with the right hand side given by (2).

Since the function f is constant on each conductor surface, it follows that u is constant in the interior of each conductor and that the gradient vanishes on the conductor surfaces when approached from the inside. From the jump relation of the normal derivative of the single-layer potential it then follows that

$$\frac{\partial u}{\partial n}(x) = \frac{1}{2}\sigma(x) + \int_S \frac{\partial}{\partial n_x} G(x,y)\sigma(y)\,dS_y = 0\,, \quad x \in S\,. \tag{5}$$

We will also write the above equation symbolically as $(1/2+\mathcal{K}')\sigma = 0$, where the operator $\mathcal{K}'$ is the adjoint of the double-layer or dipole potential $\mathcal{K}$ with respect to the L_2-inner product. The nullspace of $1/2+\mathcal{K}$ is spanned by the functions which are constant on each conductor surface

$$\mathcal{N}(1/2+\mathcal{K}) = \mathrm{span}[\chi_1, \dots, \chi_n]\,, \tag{6}$$

see [11]. Therefore we may conclude from Fredholm theory that the nullspace of $1/2+\mathcal{K}'$ is also n-dimensional and that

$$\mathcal{R}(1/2+\mathcal{K}')^{\perp} = \mathrm{span}[\chi_1, \dots, \chi_n]\,. \tag{7}$$

The capacitance problem is equivalent to finding the density σ in the null space of $1/2+\mathcal{K}'$ whose potential on conductor S_k is given by p_k.

To obtain a nonsingular second-kind integral equation select points x_k in the inside of each of the n conductors and define the operators $\mathcal{A}:\mathbb{R}^n \to C(S)$ and $\mathcal{G}:\mathbb{R}^n \to C(S)$ by

$$\begin{aligned} \mathcal{A}q(x) &= \sum_k \frac{q_k}{\sqrt{|S_k|}}\chi_k(x)\,, \quad x \in S\,, \\ \mathcal{G}q(x) &= \sum_k q_k G(x_k, x)\,, \quad x \in S\,. \end{aligned}$$

Here $C(S)$ denotes the space of continuous functions on S. The adjoints of $\mathcal{A}$ and $\mathcal{G}$ are then given by

$$\begin{aligned} [\mathcal{A}'\sigma]_k &= \frac{1}{\sqrt{|S_k|}}\int_{S_k}\sigma(y)\,dS_y\,, \\ [\mathcal{G}'\sigma]_k &= \int_S G(x_k,y)\sigma(y)\,dS_y\,. \end{aligned}$$

With the above defined operators we are able to formulate a well-posed modification of equation (5).

Theorem 2.1 *The second-kind integral equation*

$$(1/2+\mathcal{K}'+\mathcal{A}\mathcal{G}')\sigma = \mathcal{A}p\,. \tag{8}$$

is uniquely solvable. Furthermore, the solution of (8) also solves (1) when the right hand side given by (2).

Proof: To show unique solvability of equation (8) it suffices to demonstrate injectivity of operator $1/2+\mathcal{K}'+\mathcal{A}\mathcal{G}'$. For that, consider a solution σ_0 of (8) for a vanishing right hand side. Since $\mathcal{A}\mathcal{G}'\sigma_0$ is constant on each conductor it follows from (7) that $(1/2+\mathcal{K}')\sigma_0 = 0$ and that $\mathcal{A}\mathcal{G}'\sigma_0 = 0$. Thus the single-layer potential $v(x) = \mathcal{V}\sigma_0(x)$ solves the boundary value problem

$$\begin{aligned} \Delta v(x) &= 0\,, \quad x \in \mathbb{R}^3 \setminus S\,, \\ \frac{\partial v}{\partial n}^{-}(x) &= 0\,, \quad x \in S\,, \\ v(x_k) &= 0\,, \quad k = 1,\ldots,n\,. \end{aligned}$$

Hence $v \equiv 0$ and it follows that $\sigma_0 = 0$.

For the solution σ of (8) orthogonality in (7) implies that $(1/2+\mathcal{K}')\sigma = 0$ and that $\mathcal{A}\mathcal{G}'\sigma = p_k$, $k = 1,\ldots,n$. Thus the single-layer potential $\mathcal{V}\sigma(x)$ is constant within the conductors and assumes the given values on the conductor surfaces. Hence σ is the solution of (1). $\square$

The spectrum of the operator $1/2 + \mathcal{K}'$ accumulates only at $1/2$ and adding the term $\mathcal{A}\mathcal{G}'$ removes the non-trivial nullspace. Thus the eigenvalues of the operator in (8) are bounded away from zero and its inverse is a bounded operator. In practice, it is important that the norm of the inverse is small and this can become a problem in some cases. The added term not only removes the zero eigenvalues but also changes the other eigenvalues of $1/2 + \mathcal{K}'$. To weaken this effect we will also consider preconditioning of the term $\mathcal{A}\mathcal{G}'$. By repeating the arguments we used in the proof of Theorem 2.1 it can be seen that for any nonsingular $n \times n$ matrix B integral equation

$$(1/2 + \mathcal{K}' + \mathcal{A}B\mathcal{G}')\sigma = \mathcal{A}Bp \tag{9}$$

is well-posed and provides the solution of the capacitance problem.

2.1 Integral formulation involving Lagrange multipliers

An alternative way to remove the nullspace of (5) is to add the orthogonal projector into $\mathcal{R}(1/2 + \mathcal{K}')^{\perp}$

$$(1/2 + \mathcal{K}' + \mathcal{A}\mathcal{A}')\sigma = \mathcal{A}q\,. \tag{10}$$

For any vector q the solution lies in $\mathcal{N}(1/2 + \mathcal{K}')$ and it remains to determine this vector to obtain the solution of the capacitance problem. For that, consider the scalars $q_1, \ldots, q_n$ as additional unknowns. Given these extra degrees of freedom, we may require that the solution of (10) generates the given potentials inside the conductors. Thus we obtain the system

$$\begin{bmatrix} 1/2 + \mathcal{K}' + \mathcal{A}\mathcal{A}' & -\mathcal{A} \\ \mathcal{G}' & 0 \end{bmatrix} \begin{bmatrix} \sigma \\ q \end{bmatrix} = \begin{bmatrix} 0 \\ p \end{bmatrix}. \tag{11}$$

It is interesting to remark that this is the adjoint of an integral formulation for the exterior Dirichlet problem discussed by Greenbaum et al. [1] and by Mikhlin [11]. Finally, the system can be preconditioned with any two non-singular $n \times n$ matrices B_1 and B_2

$$\begin{bmatrix} 1/2 + \mathcal{K}' + \mathcal{A}B_1\mathcal{A}' & -B_1\mathcal{A} \\ B_2\mathcal{G}' & 0 \end{bmatrix} \begin{bmatrix} \sigma \\ q \end{bmatrix} = \begin{bmatrix} 0 \\ B_2 p \end{bmatrix}. \tag{12}$$

without changing the solution.

3 Discretizations

Although the numerical analysis of second-kind integral formulations is well understood, the form of equations (8) and (11) requires special care for their discretization. We describe some of these issues in this section.

The framework used here is standard and has been described by many authors, e.g. [4]. Assume that the surface S can be partitioned into finitely many patches $S = \widehat{S}_1 \cup \ldots \cup \widehat{S}_L$ where each patch $\widehat{S}_l$ is the image $x = F_l(t)$ defined on a triangular parameter domain $P_l \subset \mathbb{R}^2$. Then a family of triangulations can be obtained by uniformly refining each P_l. Let $\widehat{\Delta}_i$ be a triangle in the refinement of P_l with vertices $\widehat{v}_0, \widehat{v}_1, \widehat{v}_2$ and maximal side length h. Denote by $\Delta = \{(t_1, t_2) : 0 \leq t_1, t_2, t_1 + t_2 \leq 1\}$ the standard simplex in $\mathbb{R}^2$. Define

$$m_i(t) = F_l\left((1 - t_1 - t_2)\widehat{v}_0 + t_1\widehat{v}_1 + t_2\widehat{v}_2\right), \quad t = (t_1, t_2) \in \Delta\,,$$

and let Δ_i be the image under this mapping. The space of functions that are piecewise constant on the subdivision $S = \Delta_1 \cup \ldots \cup \Delta_N$ is denoted by X_h. The collocation points are the images of the centroids, that is, $\xi_i = m_i(\bar{t})$, where $\bar{t} = (1/3, 1/3)$. The corresponding interpolation operator $\mathcal{I}_h : C(S) \to X_h$ is then given by

$$\mathcal{I}_h f(x) = f(\xi_i)\,, \quad x \in \Delta_i\,.$$

The collocation method for the adjoint formulation (9) seeks the numerical solution σ_h^c in X_h which satisfies the integral equation at the points ξ_i

$$(1/2 + \mathcal{I}_h\mathcal{K}' + \mathcal{A}B\mathcal{G}')\sigma_h^c = \mathcal{A}Bp\,.$$

Subtracting the continuous equation (9) from its discretization leads to an expression for the error $e_h^c = \sigma - \sigma_h^c$

$$(1/2 + \mathcal{I}_h\mathcal{K}' + \mathcal{A}B\mathcal{G}')e_h^c = (\mathcal{I}_h - \mathcal{I})\mathcal{K}'\sigma = 1/2(\mathcal{I} - \mathcal{I}_h)\sigma\,.$$

Because of the compactness of the adjoint integral operator, $\mathcal{I}_h\mathcal{K}'$ converges to $\mathcal{K}'$ uniformly and hence we may estimate the collocation error by

$$\|e_h^c\|_\infty \leq \left\|(1/2 + \mathcal{K}' + \mathcal{A}B\mathcal{G}')^{-1}\right\|_\infty \|(\mathcal{I} - \mathcal{I}_h)\sigma\|_\infty\,.$$

Assuming that σ is sufficiently smooth, the error is of order h. For a finite grid the constant matters and the above estimate suggests that this factor depends critically on a good choice of the matrix B. However, this requires some a-priori knowledge of the solution which is usually not available.

The difficulty to find an appropriate B does not arise in the Galerkin method and we will demonstrate this below. Denoting the L_2-orthogonal projector into X_h by $\mathcal{P}_h$, the Galerkin discretization of (9) assumes the form

$$(1/2 + \mathcal{P}_h \mathcal{K}' + \mathcal{A}B\mathcal{G}')\sigma_h^g = \mathcal{A}Bp\,. \tag{13}$$

The projector $\mathcal{P}_h$ is self-adjoint and hence we have for all functions $\rho_h \in X_h$ and $k = 1, \ldots, n$ the identity

$$\langle \chi_k, (1/2 + \mathcal{P}_h \mathcal{K}')\rho_h \rangle = \langle \mathcal{P}_h \chi_k, (1/2 + \mathcal{K}')\rho_h \rangle = \langle \chi_k, (1/2 + \mathcal{K}')\rho_h \rangle = 0\,,$$

where $\langle .\,,. \rangle$ denotes the usual L_2 inner product. Thus $\mathcal{R}(1/2 + \mathcal{P}_h\mathcal{K}')^\perp \supset \mathrm{span}[\chi_1, \ldots, \chi_n]$ and equality holds if h is sufficiently small because of the uniform convergence of $P_h\mathcal{K}' \to \mathcal{K}'$. Hence we see from (13) that the Galerkin solution satisfies

$$\begin{aligned} (1/2 + \mathcal{P}_h\mathcal{K}')\sigma_h^g &= 0\,, \\ B\mathcal{G}'\sigma_h^g &= Bp\,. \end{aligned}$$

Therefore the solution σ_h^g is independent of B and the constant factor in the asymptotic convergence of the Galerkin error e_h^g is given by the optimal choice of this matrix. That is,

$$\left\| e_h^g \right\|_\infty \le \kappa \left\| (\mathcal{I} - \mathcal{P}_h)\sigma \right\|_\infty\,,$$

where

$$\kappa = \inf_B \left\| (1/2 + \mathcal{K}' + \mathcal{A}B\mathcal{G}')^{-1} \right\|_\infty\,.$$

The matrix coefficients of the Galerkin method are of the form

$$(K_h^g)_{ij} = \frac{1}{\alpha_i} \int_{\Delta_i} \int_{\Delta_j} \frac{\partial}{\partial n_x} G(x, y)\, dS_y\, dS_x\,, \tag{14}$$

where α_i is the surface area of panel Δ_i. To avoid the double integrals replace the integration over Δ_j by the midpoint quadrature rule (replacing Δ_i would yield the collocation method). The result is a qualocation scheme of the form

$$(\frac{1}{2} + D_h^{-1} K_h^T D_h + A_h B G_h^T)\sigma_h^q = A_h B p\,. \tag{15}$$

The matrices K_h, G_h, A_h and D_h in the above system are given by

$$(K_h)_{ij} \;=\; \int_{\Delta_j} \frac{\partial}{\partial n_y} G(\xi_i, y)\, dS_y\,, \tag{16}$$

$$(G_h)_{ik} = \int_{\Delta_i} G(x, x_k)\, dS_x\,, \tag{17}$$

$$(A_h)_{kj} = \begin{cases} 1/\sqrt{|S_k|} & \text{if } \xi_j \in S_k\,, \\ 0 & \text{else}\,, \end{cases} \tag{18}$$

$$D_h = \operatorname{diag}(\alpha_1, \ldots, \alpha_N)\,. \tag{19}$$

Note that matrix K_h arises when discretizing the double-layer operator with the collocation method. From equation (6) it follows that the nullspace of the matrix $1/2 + K_h$ is given by the vectors $\operatorname{span}[\chi_{1,h} \ldots, \chi_{n,h}]$. Thus $\mathcal{R}(1/2 + K_h^T)^\perp = \operatorname{span}[\chi_{1,h}, \ldots, \chi_{n,h}]$ and the independence of the solution σ_h of (15) from the matrix B follows as for the Galerkin method.

The error of the Galerkin method is of order h and it is important to verify that the approximation of integral (14) does not affect the asymptotic convergence. This is demonstrated in the following theorem.

Theorem 3.1 *The error $\widetilde{e}_h = \sigma_h^g - \sigma_h^q$ converges linearly, i.e.,*

$$\|\widetilde{e}_h\|_\infty = \mathcal{O}(h)\,. \tag{20}$$

Proof: Subtract equations (13) and (15). This results in the expression

$$\left(\frac{1}{2} + D_h^{-1} K_h^T D_h + A_h B G_h^T\right) \widetilde{e}_h = \left(D_h^{-1} K_h^T D_h - K_h^g\right) \sigma_h^g\,. \tag{21}$$

Set $E_h = D_h^{-1} K_h^T D_h - K_h^g$. The proof is based on showing that

$$\|E_h\|_\infty = \max_i \sum_j |E_{ij}| = \mathcal{O}(h)\,, \tag{22}$$

where $\|.\|_\infty$ is the matrix ∞-norm. With that, we have stability and linear convergence of $\|\widetilde{e}_h\|_\infty$ in (21). To demonstrate estimate (22) set

$$F_{ij}(s) = \frac{1}{4\pi} \int_\Delta \frac{D_1 \times D_2 m_i(t)^T \,(m_i(t) - m_j(s))}{|m_i(t) - m_j(s)|^3}\, dt\,, \quad s \in \Delta \tag{23}$$

then

$$E_{ij} = \frac{1}{\alpha_i} \int_\Delta (F_{ij}(\bar{s}) - F_{ij}(s))\, J_j(s)\, ds\,, \tag{24}$$

where $J_j(s) = |D_1 \times D_2 m_j(s)|$. Since the surface S is smooth, there is a constant $c > 0$ such that

$$\frac{\partial}{\partial n_x} G(x, y) \leq c\, \frac{1}{|x - y|} \quad x, y \in S\,. \tag{25}$$

For a fixed index i let

$$\mathcal{N}_l = \{ j \ : \ lh < \operatorname{dist}(\Delta_i, \Delta_j) \le (l+1)h \} \, , \quad l = 0, \ldots, \mathcal{O}(1/h) \, .$$

Because of the uniform refinement scheme, one sees easily that $\#\mathcal{N}_l \le c' l$, where c' is independent of the index i. From the chain rule and estimate (25) we have for all $j \in \mathcal{N}_l$

$$\|F_{ij}\|_\infty = \mathcal{O}(\frac{h}{l}) \, , \quad \left\|F'_{ij}\right\|_\infty = \mathcal{O}(\frac{h}{l^2}) \, , \quad \left\|F''_{ij}\right\|_\infty = \mathcal{O}(\frac{h}{l^3}) \, ,$$

and furthermore

$$\|J_j\|_\infty = \mathcal{O}(h^2) \, , \quad \left\|J'_j\right\|_\infty = \mathcal{O}(h^3) \, ,$$

where $\|.\|_\infty$ is understood componentwise for matrices and vectors. Taylor expanding the integrand in (24) about the centroid $\bar{s}$ yields

$$E_{ij} = \frac{1}{\alpha_i} \left(\int_\Delta a^T (s - \bar{s}) \, ds \, - \, \int_\Delta (s - \bar{s})^T A \, (s - \bar{s}) \, ds \, + \, r_h \right)$$

where $a = -F'_{ij}(\bar{s})$, $A = F''_{ij}(\bar{s}) J(\bar{s}) + 2 F'_{ij}(\bar{s}) J'(\bar{s})^T$ and $r_h = \mathcal{O}(h/l^4)$. The first term in the above expansion cancels out and we are left with

$$|E_{ij}| = \mathcal{O}(\frac{h}{l^3}) + \mathcal{O}(\frac{h^2}{l^2}) \, , \quad j \in \mathcal{N}_l \, ,$$

Thus the contribution to $\|E_h\|_\infty$ of panels at a positive distance can be estimated by

$$\sum_{l>0} \sum_{j \in \mathcal{N}_l} |E_{ij}| = \sum_{l>0} \mathcal{O}(\frac{h}{l^2} + \frac{h^2}{l}) = \mathcal{O}(h) \, . \tag{26}$$

It remains to estimate the contribution of nearby panels $\mathcal{N}_0$. From definition (23) it follows that $\|F_{ij}\|_\infty = \mathcal{O}(h)$ for $j \in \mathcal{N}_0$ and hence

$$|E_{ij}| \le 2 \frac{\alpha_j}{\alpha_i} \|F_{ij}\|_\infty = \mathcal{O}(h) \, , \quad j \in \mathcal{N}_0 \, .$$

Since the number of panels in $\mathcal{N}_0$ can be bounded independently of h and i, their contribution to $\|E_h\|_\infty$ is $\mathcal{O}(h)$. Together with estimate (26) assertion (22) follows. □

To facilitate numerical calculations, one often replaces integrals over triangular pieces by integrals over flat triangles. In this case there are analytical expressions of the matrix entries (16) available, see [14]. Using the techniques of Atkinson and Chien [5], it can be shown that this procedure does not change the asymptotic behavior of the error. Since the detailed proof is quite complex we do not demonstrate this here.

Finally, we remark that the discretization of the integral equation which contains the Lagrange multipliers can be treated analogously as described above for the adjoint formulation. In particular, the qualocation discretization error of equation (12) is independent of the matrices B_1 and B_2 .

4 Multipole Acceleration

We consider solving the discretized linear systems with an iterative Krylov subspace solver like GMRES of Saad and Schultz [16]. In the iteration the major numerical effort is spent in calculating matrix-vector products, which in the context considered here is equivalent to calculating the electrostatic potential due to a charge distribution. Since every panel interacts with every panel, the matrices are dense and the direct calculation of the potential involves $\mathcal{O}(N^2)$ operations.

The Fast Multipole Method (FMM) [15] is a scheme to compute N potentials due to N charges in $\mathcal{O}(N)$ operations. A detailed description for three-dimensional particle distributions has been given by Greengard [7], and the adaptation of the algorithm for collocation schemes of integral equations in 3-D potential theory by Nabors et al. [12]. This section discusses the modifications of the FMM for the qualocation scheme described in the previous section.

The FMM achieves its efficiency by using a hierarchical partition of the problem domain into cubes. The top level cube is chosen to contain all charges and is recursively subdivided until the bottom level cubes contain at most a fixed number of charges. The interactions between well-separated cubes is approximated with truncated multipole expansions.

At the bottom level the potential Φ due to charges in a cube is expanded into the truncated multipole expansion

$$\Phi(r,\theta,\phi) \approx \sum_{n=0}^{l} \sum_{m=-n}^{n} \frac{Y_n^{-m}(\theta,\phi)}{r^{n+1}} \mu_n^m . \tag{27}$$

Here r, θ, and ϕ are the spherical coordinates with respect to the multipole expansions origin (usually the center of a cube) and the $Y_n^m(\theta,\phi)$'s are the surface spherical harmonics [9]. The approximation can be made arbitrarily accurate outside the cube by increasing the expansion order l.

Once the multipole coefficients μ_n^m have been formed for every bottom level cube, the upward pass calculates the multipole coefficients for every cube in the higher levels from the multipole coefficients in the level below.

In the second phase of the algorithm, the downward pass, a local expansion of the form

$$\Psi(r,\theta,\phi) \approx \sum_{n=0}^{l} \sum_{m=-n}^{n} r^n Y_n^m(\theta,\phi)\, \lambda_n^m \tag{28}$$

is formed for every cube in the hierarchy beginning at the top level and going down to the bottom level. A local expansion approximates the potential Ψ inside the cube due to charges outside the cube and its neighbors. For more details on the upward and downward pass, we refer to Greengard's thesis [7].

Finally, in the third stage of the algorithm, the potential due to all charges is calculated by evaluating the local expansions (accounting for charges far away from the evaluation point) and evaluating the potential due to nearby charges directly.

In the case of a distribution of point charges, the multipole coefficients of a bottom level cube in (27) follow immediately from the addition theorem of spherical harmonics

$$\frac{1}{|x-y|} = \sum_{n=0}^{\infty} \sum_{m=-n}^{n} r^n Y_n^m(\theta,\phi) \frac{Y_n^{-m}(\alpha,\beta)}{\rho^{n+1}}\,, \qquad |x| < |y|\ ,$$

where the spherical coordinates of the points x and y are r, ϕ, θ and ρ, α, β, respectively. With this formula one sees easily that the multipole coefficients μ of the combined potential due to charges at r_i, ϕ_i, θ_i depend linearly on their strengths q_i. In matrix notation we have

$$\mu = Q2M\, q\,,$$

where the coefficients of the transformation matrix are

$$Q2M_{(n,m),i} = r_i^n Y_n^m(\theta_i,\phi_i)\,. \tag{29}$$

Similarly, the potentials in (28) at points $(\rho_i, \alpha_i, \beta_i)$ depend linearly on the local expansion coefficients λ_n^m. The entries of the transformation matrix are given by

$$L2P_{i,(n,m)} = \frac{Y_n^{-m}(\alpha_i,\beta_i)}{\rho_i^{n+1}}\,. \tag{30}$$

The matrix-vector product in the discretization of the double-layer operator corresponds to calculating the potential due to a collection of constant-strength dipole panels. With minor modifications, the fast multipole algorithm can also be applied for this type of calculation. In this case the coefficients of the transformation matrix (29) have the form

$$Q2M_{(n,m),i} = \int_{\Delta_i} \frac{\partial}{\partial n_i} r^n Y_n^m(\theta,\phi)\, dS_{(r,\theta,\phi)} \,. \tag{31}$$

If Δ_i is replaced by a flat triangle, there are closed-form expressions for the integrals; see [12]. The upward pass, as well as the downward- and evaluation pass for the dipole panels carry over from the algorithm for point charges. In particular, the transformation of local expansions to potentials is given by (30).

Solving the linear system arising from the adjoint integral formulation (15) involves matrix-vector multiplications with the *transpose* of the dipole potential. This operation can be multipole accelerated, too. To see this, consider the i-th row of the matrix-vector product

$$[K_h^T q]_i = \sum_j q_j \int_{T_i} \frac{\partial}{\partial n_i} \frac{1}{|\xi_j - y|}\, dS_y = \int_{\Delta_i} \frac{\partial}{\partial n_i} \Phi(y)\, dS_y$$

where

$$\Phi(y) = \sum_j q_j \, \frac{1}{|\xi_j - y|} \,.$$

Thus the i-th component of the matrix-vector product is the integral of the field due to a point-charge distribution. This suggests to use the multipole algorithm for point charges to obtain the local expansion coefficients of the potential. The evaluation pass for the adjoint formulation consists of integrating the field, given by its local expansion coefficients, over the panels. Thus the transformation matrices have the form

$$\begin{aligned} Q2M_{(n,m),i} &= \frac{Y_n^{-m}(\alpha_i,\beta_i)}{\rho_i^{n+1}} \,, && (32) \\ L2P_{i,(n,m)} &= \int_{\Delta_i} \frac{\partial}{\partial n_i} r^n Y_n^m(\theta,\phi)\, dS_{(r,\theta,\phi)} \,. && (33) \end{aligned}$$

Note that the arising translation matrices for the adjoint formulation are transposes of the matrices for the dipole operator, that is,

$$\begin{aligned} Q2M_{adjoint} &= L2P_{dipole}^T \,, \\ L2P_{adjoint} &= Q2M_{dipole}^T \,. \end{aligned}$$

5 Numerical Results

To compare collocation discretizations of the first-kind integral equation (1) with the various second-kind integral formulations discussed in this paper, we carried out a variety of numerical experiments on smooth surfaces as well as on domains with edge and corner singularities.

The discretized linear systems were solved iteratively using GMRES with multipole-accelerated matrix-vector products. Our code is based on the package FASTCAP [13] with the modifications discussed in Section 4 to implement second-kind formulations. In our experiments we monitored the convergence rate of the discretization scheme as well as in the behavior of the iterative solver.

5.1 Smooth Surfaces

Smooth surfaces give rise to compact integral operators and thus the Fredholm theory provides the framework for the numerical analysis of second-kind formulations. The first problem we consider is posed on the ellipsoid

$$S = \left\{ x \in \mathbb{R}^3 \ : \ \frac{x_1^2}{4} + \frac{x_2^2}{1} + \frac{x_3^2}{9} = 1 \right\} .$$

For this geometry the charge density can be expressed in closed form using ellipsoidal coordinates [10]. Table 1 displays the errors of the charge density in the maximum norm and the errors of the capacitance. The maximum of the error was approximated by taking the difference of the calculated and exact solution at several points in each panel. The asymptotic convergence of all discretization methods appears to be of order one, however the constant factor for the first-kind formulation and the qualocation discretization of (9) is smaller than for collocation of the second-kind formulation. The results obtained from discretizing the formulation with Lagrange multipliers (12) are not significantly different and omitted. The convergence rates of the capacitance for collocation of the adjoint formulation are of order one, whereas the rates for qualocation and collocation of the first-kind formulation are faster.

Summarizing, it appears that the errors obtained by the first-kind and qualocation of the adjoint formulation are approximately equal, whereas collocation gives much poorer approximations. The results of Table 1 are shown for $B = I$ in (9) and changing this parameter has in fact some impact on the error of the collocation method.

	first-kind, colloc		second-kind, colloc		second-kind, qualoc	
Panels	L_∞-error	cap-error	L_∞-error	cap-error	L_∞-error	cap-error
48	0.3449	2.1694	0.4605	4.2897	0.4288	2.5583
196	0.2446	0.6657	0.3828	2.1627	0.3104	0.7763
768	0.1336	0.1782	0.2510	1.1226	0.1591	0.2086
3,072	0.0765	0.0456	0.1595	0.5855	0.0908	0.0553
12,288	0.0401	0.0115	0.0880	0.3005	0.0441	0.0147

Table 1: Errors of various discretization schemes for the ellipsoid. The exact value of the capacitance is 24.7056...

The advantage of the second-kind formulations over the first-kind formulation is the conditioning of the discretized systems. In Table 2 we display the GMRES iterations that were necessary to reduce the residual to 10^{-9}. The number increases when refining the mesh for the first-kind formulation but remains bounded for the second-kind formulation.

Panels	first-kind colloc	second-kind colloc	second-kind qualoc
48	6	6	6
192	21	11	12
768	27	11	12
3,072	35	11	11
12,288	43	11	11

Table 2: Iteration count for the ellipsoid

In the first example we increased the number of panels by refining the discretization, in the following example we keep the refinement fixed and increase the number of conductors. The geometry we investigate is a collection of spheres of equal radius, pseudo-randomly distributed in space as shown in Figure 1. Each sphere is discretized into 192 flat triangles.

The results demonstrate that the first-kind and the adjoint integral formulation require more GMRES iterations to converge as the number of spheres increases. The increase for the second-kind formulation is much slower and can be controlled by the choice of the preconditioner B in (15). For $B = (\mathcal{G}'\mathcal{A})^{-1}$ the iteration count is almost constant as the number of spheres increases.

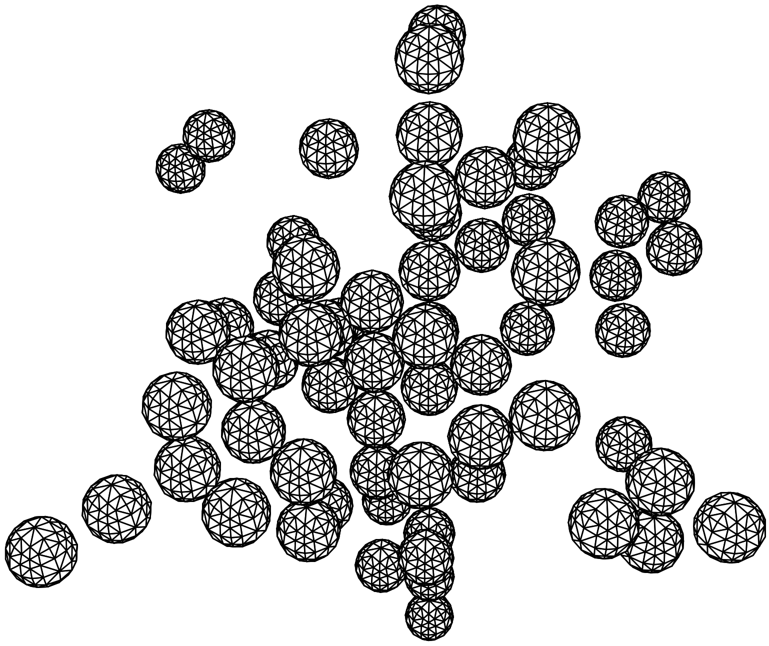

Figure 1: Sixty-four spheres example

5.2 Nonsmooth Surfaces

Although the existence theory and error analysis of the previous sections do not apply for non-smooth domains, we also include numerical results for the L-shaped block of Figure 2. The integral operator of the adjoint formulation for this domain is not compact and the charge density has corner and edge singularities. To accommodate for the poorer approximation in these regions the mesh is graded towards the singularities.

In this example the capacitance obtained by the first-kind formulation equals approximately the value obtained by the second-kind formulation on the next refinement level. Assuming that the error of the capacitance is an indicator for the error of the solution, the accuracy of the first-kind formulation appears to be better.

The number of iterations for the first-kind formulation increases when refining the mesh and the increase is faster than in the smooth case. Despite the fact that the adjoint operator is no longer compact, the iteration count for the second-kind formulation remains bounded as the grid is refined.

For edges and corners the term $1/2$ in (8) must be replaced by the solid angle, see e.g. [11]. For piecewise constant elements with centroid collocation

number spheres	first-kind	second-kind, qualoc $B = I$	$B = (\mathcal{G}'\mathcal{A})^{-1}$
4	25	13	10
8	33	21	14
16	40	28	14
32	48	31	16
64	55	32	16

Table 3: Iteration count for the multiple spheres example

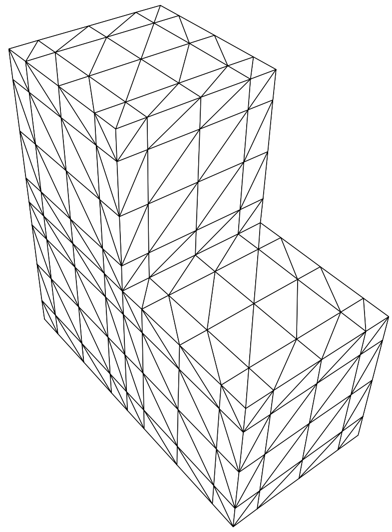

Figure 2: Discretization of the L-shaped domain

the solid angle does not appear in the discretization, because the node points lie on smooth components of the surface, and the poorer convergence of the second-kind formulation may be attributed to this missing term. On the other hand, higher order discretizations place the node points on the edges and vertices of the panels and thus solid angles appear in the discretized equation. Table 5 displays the capacitances for the L-block obtained with piecewise quadratic elements. The discretization and the matrices for this example were generated with the aid of the package BIEPACK [3].

The capacitances for the first-kind formulation apparently do not converge to the correct value, on the other hand, the capacitances of the adjoint formulation are consistent with the results obtained from using piecewise

	first-kind, colloc		second-kind, qualoc	
Panels	C_{11}	its	C_{11}	its
112	12.448	18	12.373	15
448	12.606	28	12.486	17
1792	12.650	43	12.609	20
7168	12.662	62	12.651	20
28672	12.665	87	12.662	19

Table 4: Discretization errors and GMRES iterations, L-block, piecewise constant elements

constant elements.

	first kind		second kind	
Panels	C	its	C	its
28	12.940	16	12.753	19
112	13.124	29	12.675	22
448	12.746	43	12.671	22
1792	12.742	76	12.668	22

Table 5: Capacitances and GMRES iterations, L-block, piecewise quadratic elements

6 Conclusion

Our experiments with the capacitance problem on smooth surfaces showed that second-kind formulations result in better conditioned linear systems. In addition, the adjoint formulation directly produces surface densities which are more useful in subsequent electrostatics application than the dipole layer. To maintain the accuracy of the approximation, the adjoint operator must be discretized with a non-standard qualocation scheme.

For non-smooth domains the error for piecewise constant elements is smaller for the first-kind formulation, especially for relatively coarse discretizations. However, the adjoint formulation appears to give better results then the first-kind formulation when higher order panels are used.

References

[1] A.Greenbaum, L. Greengard, and G.B. Mc Fadden. Laplace's equation and the Dirichlet-Neumann map in multiply connected domains. *J. Comput. Phys.*, 105:267–278, 1993.

[2] Kendall E. Atkinson. The numerical solution of Laplace's equation in three dimensions – II. In J.Albrecht and L.Collatz, editors, *Numerical Treatment of Integral Equations*. Birkhäuser, Basel, 1980.

[3] Kendall E. Atkinson. User's guide to a boundary elemant package for solving integral equations on piecewise smooth surfaces. *Reports on Computational Mathematics*, 43, 1993. The University of Iowa, available via anonymous ftp at `ftp.math.uiowa.edu`.

[4] Kendall E. Atkinson. *The Numerical Solution of Integral Equations of the Second Kind*. Cambridge University Press, 1997.

[5] Kendall E. Atkinson and David Chien. Piecewise polynomial collocation for boundary integral equations. *SIAM J. Sci. Statist. Comput.*, 16:651–681, 1995.

[6] L. Greengard and V. Rokhlin. A fast algorithm for particle simulations. *J. Comput. Phys.*, 73:325–348, 1987.

[7] Lesslie Greengard. *The Rapid Evaluation of Potential Fields in Particle Systems*. MIT Press, Cambridge, Massachusetts, 1988.

[8] W. Hackbusch and Z. Novak. On the fast matrix multiplication in the boundary element method by panel clustering. *Numer. Math.*, 54:463–491, 1989.

[9] E. W. Hobson. *The Theory of Spherical and Ellipsoidal Harmonics*. Chelsea Publishing Company, New York, 1965.

[10] Oliver D. Kellogg. *Foundations of Potential Theory*. Dover, New York, 1959.

[11] S. G. Mikhlin. *Integral Equations*. Pergamon Press, New York, 1957.

[12] K. Nabors, F. T. Korsmeyer, F. T. Leighton, and J. White. Preconditioned, adaptive, multipole-accelerated iterative methods for three-dimensional first-kind integral equations of potential theory. *SIAM J. Sci. Statist. Comput.*, 15(3):713–735, 1994.

[13] Keith Nabors and Jacob White. Fastcap: A multipole accelerated 3-D capacitance extraction program. *IEEE Trans. on Computer-Aided Design of Integrated Circuits and Systems*, 11(10):1447–1459, 1991.

[14] J.N. Newman. Distribution of sources and normal dipoles over a quadrilateral panel. *J. Engrg. Math.*, 20(113–126), 1986.

[15] V. Rokhlin. Rapid solution of integral equations of classical potential theory. *J. Comput. Phys.*, 60(2):187–207, 1985.

[16] Youcef Saad and Martin H. Schultz. GMRES: A generalized minimal residual algorithm for solving nonsymmetric linear systems. *SIAM J. Sci. Statist. Comput.*, 7(3):105–126, 1986.

[17] Ian Sloan. Error analysis of boundary integral methods. *Acta Numerica*, pages 287–339, 1991.